Investigation of resonance polarization phenomena during the passage of laser radiation through potassium vapor

V. M. Arutyunyan, T. A. Papazyan, Yu. S. Chilingaryan, A. V. Karmenyan, and S. M. Sarkisyan

Erevan State University

(Submitted June 30, 1973)
Zh. Eksp. Teor. Fiz. **66**, 509–519 (February 1974)

An experimental study has been carried out of the polarization properties of stimulated parametric four-photon, three-photon, and electronic Raman scattering when high-intensity polarized resonance radiation is passed through potassium vapor. A qualitative comparison is given between the amplification factors for these effects in different planes of polarization and the calculated values. A Stark shift has also been observed for the three-photon line and the SERS line in the plane of polarization of the pump wave. The effect of parametric scattering on three-photon scattering and SERS is investigated.

INTRODUCTION

Atoms exhibit considerable nonlinearity under resonance conditions. The result is that when laser radiation interacts with atomic systems, even in the gaseous state, the latter exhibit various nonlinear multiphoton effects whose intensity is comparable with that of nonlinear processes in nonresonance condensed media. The nonlinear interaction between light and alkali metal vapors has been investigated in particular detail. In the resonance situation, there is a clear high-frequency Stark effect,[1-3] resonance self-excitation,[4] self-modulation broadening of the spectrum,[5] stimulated electronic Raman scattering,[6] stimulated three-photon scattering,[3,7] and parametric three-photon scattering.[8,9]

Theoretical analysis of these effects is, as a rule based on the scalar equations for the resonance medium, and polarization is ignored. This analysis is purely qualitative and cannot explain the quantitative experimental results, or the many specific polarization effects such as the splitting and shift of levels, rotation of the polarization ellipse, splitting of lines due to multiphoton processes, and so on. The influence of polarization on a number of effects was investigated theoretically in[10,13]. In this paper we report an experimental study of resonance polarization effects, observed during the passage of laser radiation through potassium vapor, and their theoretical analysis.

1. THE POTASSIUM ATOM IN THE FIELD OF A POLARIZED WAVE

Let us consider the behavior of a potassium atom in the field of a polarized wave. The ground state of the potassium atom can be classified as $4S_{1/2}$, and the lowest excited states are $4P_{1/2}$ and $4P_{3/2}$. Figure 1 shows the disposition of these potassium levels.

Suppose that the potassium atom is placed in the field of laser radiation whose frequency differs somewhat from that indicated in Fig. 1, It is well known that the effect of the external field is to shift the energy levels and, if we recall that the dipole moments for transitions between different sublevels are different, we must conclude that the high-frequency Stark effect depends on the wave polarization. We shall confine our attention to linear and circular polarization.

Suppose that the quantization axis is parallel to the electric vector in the linearly polarized exciting wave. When this is so, the wave couples only states with equal angular momentum components m and, therefore, the $4P_{3/2}$ states with $m = \pm 3/2$ are not coupled to the ground state and are not, therefore, shifted. When $\Delta\nu' = \nu - \nu_0'$ is much greater than $\Delta\nu = \nu - \nu_0$, the effect of the $4S_{1/2} \rightarrow 4P_{1/2}$ transition on the level shift can be neglected. (In our case, $\Delta\nu' \sim 80\ \text{cm}^{-1}$, $\Delta\nu \sim 23\ \text{cm}^{-1}$). In this approximation, we can also neglect the shift of the $4P_{1/2}$ level.

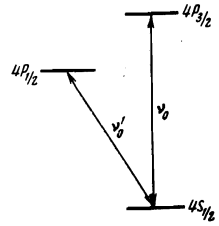

FIG. 1. Main potassium levels: $\nu_0 = 13\,043\ \text{cm}^{-1}$ and $\nu_0' = 12\,986\ \text{cm}^{-1}$.

The shifts of the upper and lower levels are both equal to ΔE, where[10]

$$\Delta E = hc\Delta\nu(\sqrt{1+\xi}-1)/2,\ \xi = 7.89\cdot 10^{-6}P/\Delta\nu^2. \qquad (1.1)$$

The numerical value of the dimensionless intensity parameter ξ is given for the $4S_{1/2} \rightarrow 3P_{3/2}$ transition in potassium and P is the wave energy density in W/cm^2.

For circular polarization, the quantization axis is conveniently taken to be parallel to the direction of propagation. Let us suppose that the wave is polarized with left-handed circular polarization. States for which $\Delta m = +1$ are then coupled and, therefore, $4P_{3/2}$ states with $m = -1/2, -3/2$ are not coupled to the ground state and are not shifted. Since the matrix element for the $+1/2 \rightarrow +3/2$ transition is greater by a factor of $\sqrt{3}$ than the matrix element for the $-1/2 \rightarrow +1/2$ transition, the level shifts ΔE_1 and ΔE_2 differ by a factor of three (in the approximation of the quadratic Stark effect), i.e.,

$$\Delta E_{1,2} = hc\Delta\nu(\sqrt{1+\xi_{1,2}}-1)/2,\ \xi_1 = \xi/2,\ \xi_2 = 3\xi/2. \qquad (1.2)$$

Figure 2 shows schematically the potassium levels in the field of the polarized wave.

2. EXPERIMENTAL SETUP AND METHOD FOR MEASURING POLARIZATION EFFECTS IN POTASSIUM VAPOR

We have investigated experimentally parametric scattering, stimulated three-photon scattering, and stimulated electronic Raman scattering. These experiments were carried out with the apparatus shown schematically in Fig. 3.

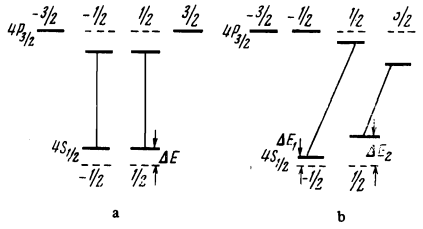

FIG. 2. Potassium atom in the field of a linearly polarized wave (a) and a wave with left-hand circular polarization (b).

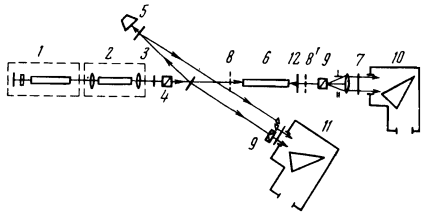

FIG. 3. Schematic arrangement of the apparatus: 1) ruby laser; 2) container with chloroform; 3) filter; 4) polarizer; 5) calorimeter; 6) container with potassium vapor; 7), 8), 8′) quarter-wave plates; 9) Wollaston prism; 10), 11) ISP-51 spectrograph; 12) transparent mirror.

The potassium vapor was illuminated with radiation of frequency $\nu \sim 13066\ cm^{-1}$ which was produced through the generation of the second Stokes component in SRS in chloroform exposed to ruby laser radiation. The SRS power density was $\sim 10\ MW/cm^2$ in the unfocused beam. This pulse was transmitted through the polarizer 4, and the filter 3 was used to eliminate the main ruby laser radiation. The potassium vapor density was varied between 5×10^{15} and 1.2×10^{16} atoms/cm^3. The interaction length, i.e., the length of the container with the vapor, was 30 cm. The two mutually perpendicular polarization components of light transmitted through the potassium vapor were separated by the Wollaston prism 9 and recorded by the spectrograph 10 with linear dispersion of 41 cm^{-1}/mm. The system can also be used to record the back wave obtained with the aid of the semitransparent mirror 12. This wave was directed onto the spectrograph 11 after passing through the vapor and was also separated into the two mutually perpendicular polarization components. In all cases, the polarization of one of the recorded components was the same as that of the exciting radiation. Quarter-wave plates 8 and 8′ were used to investigate the effects associated with the interaction between the circularly polarized light and the medium. The plate 8′ was used to analyze the right- and left-hand circles for the direct wave, and the plate 8 was used for the same purpose for the back wave. The frequency and energy were monitored throughout the experiments (the latter with the calorimeter 5).

3. PARAMETRIC FOUR-PHOTON INTERACTION

During the parametric four-photon interaction, the atom absorbs four incident photons and emits two others, in accordance with the scheme $2\nu \rightarrow \nu_1 + \nu_2$. Because of coherence, the four-photon interaction occurs in the direction of the incident radiation and leads to broadening of the spectrum. When we consider this effect, we shall at first neglect the influence of the $4S_{1/2} \rightarrow 4P_{1/2}$ transition but will take it into account later.

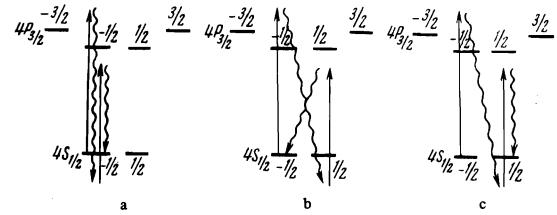

FIG. 4. Parametric scattering in the field of the linearly polarized pump wave (wavy lines show emitted photon).

FIG. 5. Scattered spectrum in the direction of the pump (linear polarization): a) scattered spectrum with polarization identical with that of the pump; b) scattered spectrum with reverse polarization.

A. Case of Linear Polarization

Figure 4 shows diagrams describing the parametric interaction in the case of linear polarization of the exciting radiation (symmetric processes obtained by inverting the signs of the angular momenta are also possible). In Fig. 4a, the emitted photons ν_1 and ν_2 have the same Z polarization as the incident radiation, whereas in Fig. 4b the scattered photons have their polarizations along Y. Parametric processes associated with different polarizations do not mix. Processes capable of mixing different polarizations are shown in Fig. 4c. Here, one of the scattered photons has the Z polarization and the other the Y polarization. However, the matrix elements for this case are identically zero if the initial $4S_{1/2}$ states with $m = -1/2$ and $m = +1/2$ are not coherent. When they are coherent (the atom is initially polarized) the analysis of the parametric processes becomes much more complicated.

Calculations show[10] that parametric scattering leads to the symmetric broadening of the spectrum relative to the incident frequency in the region

$$|\nu' - \nu| \leqslant \Delta\nu\sqrt{\xi} \tag{3.1}$$

where ν' is the frequency of the scattered photon. At the incident frequency there is no nonparametric amplification and there is a clear maximum at the frequency

$$\nu_{max} = \Delta\nu[\xi(\xi+1)/(\xi+2)]^{1/2}. \tag{3.2}$$

In the perpendicular plane, additional absorption due to $-1/2 \rightarrow -3/2$ transitions ensures that analytic results can be obtained only for $\xi \ll 1$. In particular, the region of broadening is defined by

$$|\nu' - \nu| \leqslant \Delta\nu\sqrt{\xi/2}, \tag{3.3}$$

and the frequency at the maximum is

$$\nu_{max}' = \Delta\nu\sqrt{\xi/2}/2. \tag{3.4}$$

Figure 5 shows the spectrogram for the radiation transmitted by potassium vapor. As can be seen, the incident radiation is strictly linearly polarized (this can be judged by examining the first Stokes SRS component in chloroform). The second Stokes component is appreciably broadened in both planes, and the broadening is greater in the Z plane.

The determination of the parametric line contour in the Z and Y planes is highly complicated by the presence of the incident line (in the Y plane it appears as a result of rotation). Nevertheless, we have succeeded in

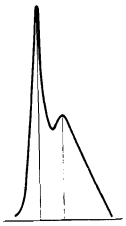

FIG. 6. Microphotogram of the broadened line in the Y plane.

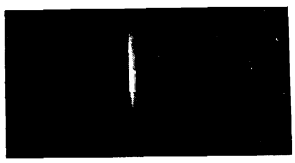

FIG. 7. Spectrum of parametric scattering (the parametric scattering maximum is seen on the right).

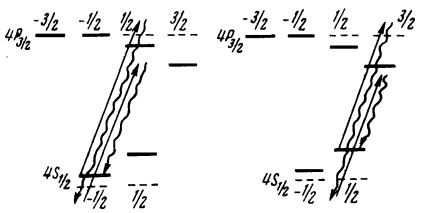

FIG. 8. Parametric scattering in the field of the pump wave with left-hand circular polarization between the sublevels $+1/2 \rightarrow -1/2$ (a) and $+3/2 \rightarrow -1/2$ (b).

detecting the maximum given by (3.2) in a number of cases.

Figure 6 gives a microphotogram of the broadened line in the Y plane, which clearly shows the presence of the above maximum. The parametric effect appears in its pure form when the angular distribution of the scattered radiation is investigated.

It is clear from Fig. 7 that there is no amplification at the incident line outside the excitation cone, and the maximum of the parametric emission spectrum is shifted relative to the exciting radiation.

B. Case of Circular Polarization

Figure 8 illustrates the parametric interaction between a wave with left-hand polarization and a potassium atom. It is clear from this figure that the parametrically scattered photons are polarized in the same way as the incident radiation. Therefore, there is no broadening for the right circle. The broadening region in this case is given by

$$|\nu'-\nu| \leqslant \Delta\nu \sqrt{5\xi_1/2}. \qquad (3.5)$$

The spectrograms of the transmitted radiation (Fig. 9) clearly show that the broadening occurs only for circular polarizations which are the same as the polarization of the incident radiation.

C. Effect of the $4S_{1/2} \rightarrow 4P_{1/2}$ Transition on Parametric Scattering

Analysis of the parametric four-photon scattering in potassium vapor is usually restricted to the two-level approximation, and only the resonance $4S_{1/2} \rightarrow 4P_{3/2}$ transition is taken into account. This is usually justified by the fact that the incident radiation is in resonance with this transition. In reality, this is not correct when the frequency of the parametrically scattered photon is near ν_0'.

FIG. 9. Scattered spectrum in the direction of the pump (circular polarization): a) scattered spectrum with polarization identical with that of the pump; b) scattered spectrum with reverse circular polarization.

FIG. 10. Spectrogram of radiation transmitted by potassium vapor.

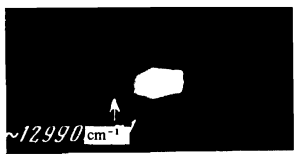

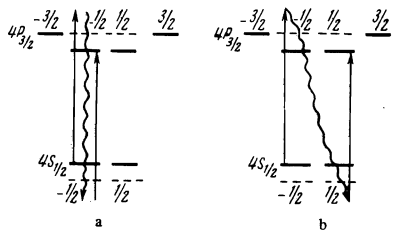

FIG. 11. Three-photon scattering in the field of a linearly polarized wave: a) scattered photon has the same polarization as the pump; b) scattered photon has perpendicular polarization.

The conservation of energy and momentum in the parametric process in the direction of the incident radiation is described by

$$2\nu = \nu_1 + \nu_2, \quad 2\nu n(\nu) = \nu_1 n(\nu_1) + \nu_2 n(\nu_2), \qquad (3.6)$$

where the refractive index of the medium is given by

$$n(\nu) = 1 + \frac{P_1/4\pi^2}{\nu(\nu_0 - \nu)} + \frac{P_2/4\pi^2}{\nu(\nu_0' - \nu)}. \qquad (3.7)$$

It follows from (3.6) and (3.7) that there is an additional parametric interaction near the frequencies

$$\nu' = \nu \pm \Delta\nu' \left[\frac{1+\eta(\Delta\nu/\Delta\nu')^3}{1+\eta(\Delta\nu/\Delta\nu')}\right]^{1/2} \qquad (3.8)$$

where $\eta \approx 0.5$ is the ratio of the oscillator strengths for the $4S_{1/2} \rightarrow 4P_{1/2}$ and $4S_{1/2} \rightarrow 4P_{3/2}$ transitions. It is clear from (3.8) that the frequency of the scattered radiation depends only on the incident frequency and the ratio of the oscillator strengths. Figure 10 shows the spectrogram in which the parametric line (3.8) is clearly seen. In the experiment, ν' was varied from pulse to pulse, which correlated with the random changes in the frequency of the excited radiation. Equation (3.8) also leads us to expect a symmetric line on the short-wave side, but we have not succeeded in observing it. A more detailed theoretical analysis of the amplification coefficients at these frequencies shows that this line is narrower by an order of magnitude as compared with the usual parametric line.[12]

4. STIMULATED THREE-PHOTON SCATTERING

In the case of three-photon scattering, the atom absorbs two incident photons of frequency ν, emits a photon of frequency $\nu_S = 2\nu - \nu_0$, and is left in an excited state. Let us consider this process with allowance for polarization.

A. Case of Linear Polarization

Three-photon processes are shown schematically in Fig. 11. Figure 11a corresponds to three-photon scattering with Z-polarized pump (a similar situation oc-

TABLE I

Transition	Polarization of the three-photon radiation	Frequency	Gain factor
$-\frac{1}{2}\to-\frac{1}{2}$ $+\frac{1}{2}\to+\frac{1}{2}$	Z	$\nu_s=\nu+$ $+\Delta\nu\sqrt{1+\xi}$	$g_Z(\nu_s)$
$-\frac{1}{2}\to+\frac{1}{2}$ $+\frac{1}{2}\to-\frac{1}{2}$	Y	$\nu_s=\nu+$ $+\Delta\nu\sqrt{1+\xi}$	$g_Y(\nu_s)$

* where $g_Z(\nu_s)=4g_Y(\nu_s)=\pi q\Delta\nu\frac{(\sqrt{1+\xi}-1)^2}{1+\xi}\delta(\nu'-\nu_s')$.

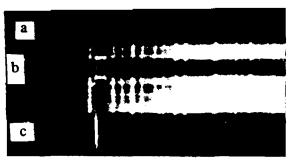

FIG. 12. Scattered spectrum in the direction opposite to that of the direction of propagation of the pump wave (linearly polarized pump): a) the Y polarization plane perpendicular to the Z polarization plane of the pump: b) pump wave polarized in the Z plane; c) pump spectrum.

curs for $+1/2\to+1/2$ transitions) and Fig. 11b corresponds to the photon with perpendicular Y polarization (the $+1/2\to-1/2$ transition occurs with the same probability).

Table I shows the gain factors $g(\nu')$ for different transitions, and it is clear that

$$g_z(\nu_s):g_Y(\nu_s)=4:1. \tag{4.1}$$

Three-photon scattering in the case of linear polarization has also been observed in the reverse direction (Fig. 12). Three-photon scattering is suppressed in the direction of the exciting radiation because of parametric effects[5,7].

In all cases, we observed only the three-photon scattering with Z polarization (polarization of the incident radiation). This is apparently connected with the fact that, according to (4.1), the gain for the Z polarization is greater by a factor of four than for the Y polarization and in the reverse direction there is an exponential law of amplification. The experiments clearly show the Stark shift which, in some cases, amounts up to 7 cm^{-1}. This corresponds to a pump density of ~60 MW/cm^2. This magnitude of the shift can only be explained by the self-focusing of the pump radiation,[4,14] since in our experiments the maximum power density at entry into the container did not exceed 15 MW/cm^2. Self-focusing can also explain the absence of correlation between the Stark shift and the measured power density at entrance into the container.

B. Case of Circular Polarization

In this case, three-photon scattering processes can occur only for the $-1/2\to+1/2$ and $+1/2\to+3/2$ transitions (left-hand pump polarization). It is clear that the scattered photons have the polarization of the pump, but frequencies are different for the first and second cases. Table II shows the frequencies and gain factors in these cases, where it is clear that for $\xi\ll1$

$$g(\nu''_{s(-)}):g(\nu'_{s(-)})=27:1. \tag{4.2}$$

In experiments with a circularly polarized pump, we observed the three-photon line with the same polarization. The three-photon line with the opposite polarization was not observed in this case (see Fig. 16).

TABLE II

Transition	Polarization of the three-photon radiation	Frequency	Gain factor
$-\frac{1}{2}\to+\frac{1}{2}$	Left-handed	$\nu'_{s(-)}=\nu+$ $+\Delta\nu\sqrt{1+\xi_1}$	$g(\nu'_{s(-)})$
$+\frac{1}{2}\to+\frac{3}{2}$	Left-handed	$\nu''_{s(-)}=\nu+$ $+\Delta\nu\sqrt{1+\xi_2}$	$g(\nu''_{s(-)})$

* where $g(\nu'_{s(-)})=\frac{\pi q\Delta\nu}{2}\frac{(\sqrt{1+\xi_1}-1)^2}{1+\xi_1}\delta(\nu'-\nu'_{s(-)})$,
$g(\nu''_{s(-)})=\frac{3\pi\Delta\nu q}{2}\frac{(\sqrt{1+\xi_2}-1)^2}{1+\xi_2}\delta(\nu'-\nu''_{s(-)})$.

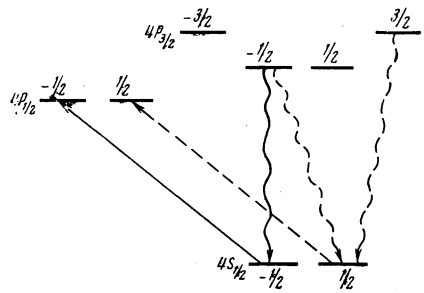

FIG. 13. The SERS processes in the field of a linearly polarized wave. The solid wavy line corresponds to the emitted SERS photon in the Z polarization plane, and the broken lines correspond to the Y polarization plane.

5. STIMULATED ELECTRONIC RAMAN SCATTERING (SERS)

The three-photon scattering and absorption processes result in the population of the $4P_{3/2}$ state and this leads to the appearance of an inversion between the $4P_{3/2}$ and $4P_{1/2}$ states. This means that stimulated electronic Raman scattering with frequency $\nu_R=\nu+\Delta$ becomes possible where $\Delta=\nu_0-\nu_0'$.

Since the Raman frequency is close to ν_0 and ν_0', we can confine our attention to the levels shown in Fig. 1.

A. Case of Linear Polarization

Figure 13 shows the diagrams for SERS processes in the field of a linearly polarized wave. Table III shows the possible transitions and frequencies for all these processes. We do not give the gain factors because they depend on the particular population of the $4P_{3/2}$ sublevels. When all the sublevels are equally populated, we should have

$$g_z(\nu_R):g_Y(\nu_R):g_Y(\nu_R')=4:1:3. \tag{5.1}$$

Figure 14 gives the back-wave spectrum, showing clear SERS lines both in the Z and Y polarization planes. The SERS lines in different planes are shifted relative to one another. Experiments show that the shifted SERS line is absent from the Y plane, and this is in good agreement with (5.1). The position of the unshifted line agrees with $\nu_R'=\nu+\Delta$ where $\Delta=57$ cm^{-1} to within experimental error. As expected, the SERS line in the Z plane is shifted, and the maximum observed shift is of the order of 3 cm^{-1}. The SERS line shift should be smaller by a factor of two than the three-photon line, but because of the difference in the gain factors under our experimental conditions the three-photon line was so broadened that the simultane-

TABLE III

Transition	Polarization	Frequency
$+\frac{1}{2}\rightarrow+\frac{1}{2}$; $-\frac{1}{2}\rightarrow-\frac{1}{2}$	Z	$\nu_R=\nu+\Delta-\Delta\nu(\sqrt{1+\xi}-1)/2$
$-\frac{1}{2}\rightarrow+\frac{1}{2}$; $+\frac{1}{2}\rightarrow-\frac{1}{2}$	Y	$\nu_R=\nu+\Delta-\Delta\nu(\sqrt{1+\xi}-1)/2$
$-\frac{3}{2}\rightarrow-\frac{1}{2}$; $+\frac{3}{2}\rightarrow+\frac{1}{2}$	Y	$\nu'_R=\nu+\Delta$

FIG. 14. The scattered spectrum in the direction opposite to that of the pump (linearly polarized pump): a) the plane of polarization Y is perpendicular to the plane of polarization of the pump wave Z; b) pump wave polarized in the Z plane; c) pump spectrum.

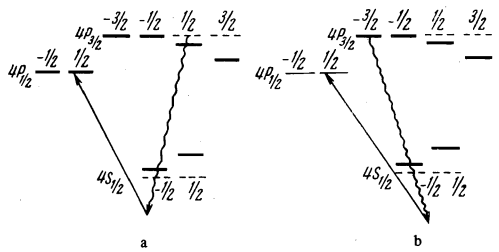

FIG. 15. Possible SERS processes between different sublevels in the case of pump wave with left-hand circular polarization.

ous determination of both shifts was impossible. Nevertheless, on the average, the SERS line shift was smaller by a factor of two than the shift of the three-photon line.

B. Case of Circular Polarization

Processes which lead to SERS in the case of a circularly polarized pump are shown schematically in Fig. 15, and Table IV shows the corresponding transitions and frequencies. When the populations of the $+1/2$ and $-3/2$ levels are equal

$$g(\nu_{R(-)}):g(\nu_{R(+)})=1:3. \qquad (5.2)$$

When the pump wave is 100% left-hand polarized, the $-3/2$ sublevel is not populated. However, a small linear polarization impurity in our experiment (Fig. 16) enabled us to detect the line at $\nu_{R(+)}$ (right-hand circular polarization without Stark effect). The ratio of the observed intensities for different polarization circles is not inconsistent with (5.2). The spectrogram given in Fig. 16 shows also the three-photon line with the same polarization circle.

As already noted, four-photon scattering occurs in the direction of the pump within the limits of a narrow cone and, therefore, does not affect the character of the three-photon scattering process in the back direction. The cross section for the four-photon scattering process has a clearly defined maximum when $\nu_1=\nu_0$, $\nu_2=2\nu-\nu_0$, i.e., near the three-photon scattering and atomic-absorption frequencies. It is shown in[10] that this leads to a sharp suppression of three-photon scattering and absorption processes in the direction of the pump. This

TABLE IV

Transition	Polarization	Frequency
$+\frac{1}{2}\rightarrow+\frac{1}{2}$	Left-handed	$\nu_{R(-)}=\nu+\Delta-\Delta\nu(\sqrt{1+\xi_\perp}-1)/2$
$-\frac{3}{2}\rightarrow+\frac{1}{2}$	Right-handed	$\nu_{R(+)}=\nu+\Delta$

FIG. 16. Scattered spectrum in the back direction (circularly polarized pump): a) scattered spectrum with the same polarization as the pump; b) scattered spectrum with opposite polarization; c) pump spectrum.

explains the termination of the population of those $4P_{3/2}$ states which participate in the parametric four-photon scattering (we note that the excited levels are populated through three-photon scattering and absorption). For example, in the case of linear polarization, the $4P_{3/2}$ sublevels with $m=\pm1/2$ are not populated. Hence, as is clear from Table III, in the direction of the pump we have only SERS corresponding to $\pm3/2\rightarrow\pm1/2$ transitions, i.e., the Raman photon is polarized at right-angles to the pump and has the frequency $\nu'_R=\nu+\Delta$ (there is no Stark effect for this line). This is clearly seen in the spectrogram given in Fig. 5. In the case of circular polarization, $4P_{3/2}$ levels with $m=+1/2$ and $m=+3/2$ participate in the parametric process and, therefore, Raman transitions from these levels must cease. When the $-3/2$ level is populated, it follows from Table IV that a Raman line should be observed in the direction of the pump, which corresponds to the $-3/2\rightarrow+1/2$ transition with the frequency $\nu_{R(+)}=\nu+\Delta$ and polarization opposite to that of the pump.

The case of pure circular polarization is illustrated in Fig. 9, which shows the absence of the SERS line (the $-3/2$ level is unpopulated in this case).

[1] A. M. Bonch-Bruevich and V. A. Khodovoĭ, Usp. Fiz. Nauk 93, 71 (1967) [Sov. Phys.-Usp. 10, 637 (1968)].
[2] A. M. Bonch-Bruevich, N. P. Kostin, V. A. Khodovoĭ, and V. V. Khromov, Zh. Eksp. Teor. Fiz. 56, 144 (1969) [Sov. Phys.-JETP 29, 82 (1969)].
[3] V. M. Arutyunyan, N. N. Nadalyan, V. A. Iradyan, and M. E. Movsesyan, Zh. Eksp. Teor. Fiz. 60, 62 (1971) [Sov. Phys.-JETP 33, 34 (1971)].
[4] D. Grischkowsky, Phys. Rev. Lett. 24, 866 (1970).
[5] V. M. Arutyunyan, N. N. Badalyan, V. A. Iradyan, and M. E. Movsesyan, Zh. Eksp. Teor. Fiz. 58, 37 (1970) [Sov. Phys.-JETP 31, 22 (1970)].
[6] P. P. Sorokin, N. S. Shiren, J. R. Lankard, E. C. Hammond, and T. G. Kazyaka, Appl. Phys. Lett., 10, 44 (1967).
[7] V. M. Arutyunyan, E. G. Kanetsyan, and V. O. Chaltykyan, Zh. Eksp. Teor. Fiz. 59, 195 (1970) [Sov. Phys.-JETP 32, 108 (1971)].
[8] Yu. M. Kirin, S. G. Rautian, A. E. Semenov, and B. M. Chernoborod, ZhETF Pis. Red. 11, 340 (1970) [JETP Lett. 11, 226 (1970)].
[9] A. M. Bonch-Bruevich, V. A. Khodovoĭ, and V. V. Khromov, ZhETF Pis. Red. 11, 431 (1970) [JETP Lett. 11, 290 (1970)].
[10] V. M. Arutyunyan, E. G. Kanetsyan, and V. O. Chaltykyan, Zh. Eksp. Teor. Fiz. 62, 908 (1972) [Sov. Phys.-JETP 35, 482 (1972)].

[11] G. G. Adonts, V. O. Chaltykyan, and N. V. Shakhnazaryan, Izv. Akad. Nauk Arm. SSR Fiz. 8, 28 (1973).
[12] G. G. Adonts, A. Zh. Muradyan, and V. G. Kolomiets, Izv. Akad. Nauk Arm. SSR Fiz. (in press).
[13] G. G. Adonts, L. Kocharyan, and N. V. Shakhnazaryan, Izv. Akad. Nauk Arm. SSR Fiz. (in press).
[14] S. A. Akhmanov, A. I. Kovrigin, S. A. Maksimov, and V. E. Ogluzdiv, ZhETF Pis. Red. 15, 186 (1972) [JETP Lett. 15, 129 (1972)].

Translated by S. Chomet
51